



Published in final edited form as:

Science. 2016 January 15; 351(6270): 271–275. doi:10.1126/science.aad4076.

A peptide encoded by a transcript annotated as long noncoding RNA enhances SERCA activity in muscle

Benjamin R. Nelson^{1,2,*}, Catherine A. Makarewich^{1,2,*}, Douglas M. Anderson^{1,2}, Benjamin R. Winders^{1,2}, Constantine D. Troupes^{3,4}, Fenfen Wu⁵, Austin L. Reese^{6,7}, John R. McAnally^{1,2}, Xiongwen Chen^{3,4}, Ege T. Kavalali^{6,7}, Stephen C. Cannon⁵, Steven R. Houser^{3,4}, Rhonda Bassel-Duby^{1,2}, and Eric N. Olson^{1,2,†}

¹Department of Molecular Biology, University of Texas Southwestern Medical Center, Dallas, TX 75390, USA

²Hamon Center for Regenerative Science and Medicine, University of Texas Southwestern Medical Center, Dallas, TX 75390, USA

³Department of Physiology, Temple University School of Medicine, Philadelphia, PA 19140, USA

⁴Department of Cardiovascular Research Center, Temple University School of Medicine, Philadelphia, PA 19140, USA

⁵Department of Neurology, University of Texas Southwestern Medical Center, Dallas, TX 75390, USA

⁶Department of Neuroscience, University of Texas Southwestern Medical Center, Dallas, TX 75390, USA

⁷Department of Physiology, University of Texas Southwestern Medical Center, Dallas, TX 75390, USA

Abstract

Muscle contraction depends on release of Ca²⁺ from the sarcoplasmic reticulum (SR) and reuptake by the Ca²⁺adenosine triphosphatase SERCA. We discovered a putative muscle-specific long noncoding RNA that encodes a peptide of 34 amino acids and that we named dwarf open reading frame (DWORF). DWORF localizes to the SR membrane, where it enhances SERCA activity by displacing the SERCA inhibitors, phospholamban, sarcolipin, and myoregulin. In mice, overexpression of DWORF in cardiomyocytes increases peak Ca²⁺ transient amplitude and SR Ca²⁺ load while reducing the time constant of cytosolic Ca²⁺ decay during each cycle of contraction-relaxation. Conversely, slow skeletal muscle lacking DWORF exhibits delayed Ca²⁺ clearance and relaxation and reduced SERCA activity. DWORF is the only endogenous peptide

[†]Corresponding author. ; Email: eric.olson@utsouthwestern.edu

*These authors contributed equally to this work.

SUPPLEMENTARY MATERIALS

www.sciencemag.org/content/351/6270/271/suppl/DC1

Materials and Methods

Figs. S1 to S17

Tables S1 to S4

References (23-36)

known to activate the SERCA pump by physical interaction and provides a means for enhancing muscle contractility.

Intracellular Ca^{2+} cycling is vitally important to the function of striated muscles and is altered in many muscle diseases. Upon electrical stimulation of the myocyte plasma membrane, Ca^{2+} is released from the sarcoplasmic reticulum (SR) and binds to the contractile apparatus triggering muscle contraction (¹). Relaxation occurs as Ca^{2+} is pumped back into the SR by the sarco-endoplasmic reticulum Ca^{2+} adenosine triphosphatase (SERCA). SERCA activity is inhibited by the small transmembrane peptides phospholamban (PLN), sarcolipin (SLN), and myoregulin (MLN; also known as MRLN) in vertebrates and by sarcolamban A and B (sclA and sclB) in invertebrates, which diminish sarcoplasmic reticulum (SR) Ca^{2+} uptake and myocyte contractility (^{2,7}).

Recently, we discovered the small open reading frame (ORF) of MLN within a transcript annotated as a long noncoding RNA (lncRNA) (⁴). We hypothesized that a subset of transcripts currently annotated as lncRNAs may encode small proteins that have evaded annotation efforts, a notion supported by recent proteomic analyses (⁸⁻¹⁰). To identify potential peptides, we searched presumably noncoding RNA transcripts for hypothetical ORFs using PhyloCSF; this method uses codon substitution frequencies (¹¹). From these transcripts, we discovered a previously unrecognized ORF of 34 codons within a muscle-specific transcript, which we call dwarf open reading frame (*Dwarf*) (fig. S1). The *Dwarf* RNA transcript is annotated as NONCODE lncRNA gene NONMMUG026737 (¹²) in mice and lncRNA LOC100507537 in the University of California, Santa Cruz, human genome (fig. S2A). With only 34 codons, DWORF is currently the third smallest full-length protein known to be encoded by the mouse genome.

The murine *Dwarf* transcript is encoded in three exons on chromosome 3 (fig. S2A). The ORF begins in exon 1, which encodes the first four amino acids of the protein, and the remaining protein is encoded in exon 2. Use of alternative splice acceptors between exons 1 and 2 produces two transcripts that differ by a three-nucleotide insertion. The ORF is conserved to lamprey, the most distant vertebrate genome available (fig. S2B), and scores positively with PhyloCSF (fig. S2C). The C terminus is hydrophobic and is predicted to encode a tail-anchored transmembrane peptide (¹³⁻¹⁵). The N terminus is less stringently conserved, but most sequences contain multiple charged residues (primarily lysine and aspartic acid) in this region. Unless otherwise noted, further studies focused on the murine homolog of DWORF.

Northern blot analysis showed that the mRNA transcript is robustly expressed in the heart (Fig. 1A). By quantitative reverse transcription polymerase chain reaction (qRT-PCR), *Dwarf* RNA was also detected in heart and soleus, a postural muscle group of the hindlimb containing the greatest enrichment of slow-twitch muscle fibers in mice (fig. S3A), as well as diaphragm, which contains some slow-twitch fibers but is primarily a fast-twitch muscle in mice (^{16, 17}). Notably, *Dwarf* was not detected in the quadriceps, a fast-twitch muscle group, or in cardiac atrial muscle. *Dwarf* is not expressed in the prenatal heart but gradually increases in abundance postnatally (fig. S3B).

Cloning of the *Dwarf* 5' untranslated region in frame with an ORF lacking a start codon efficiently initiates translation of the ORF (fig. S4). To further confirm that the transcript encodes a protein, we raised a polyclonal rabbit antibody against the N-terminal 12 amino acids of the predicted protein. Western blotting revealed a single band at the expected molecular mass of 3.8 kD in soleus and heart but not in other tissues (Fig. 1B).

Given its abundance in heart tissue, we examined whether *Dwarf* mRNA or protein expression changes in response to pathological cardiac signaling. Indeed, in mice bearing a cardiac-specific α -myosin heavy chain (α MHC) promoter driven calcineurin transgene, which serve as a model of hypertrophic heart disease that progresses to dilated cardiomyopathy by 6 months of age (¹⁸), *Dwarf* mRNA was down-regulated in dilated transgenic hearts of 6-month-old mice (Fig. 1C). Notably, DWORF protein was more dramatically down-regulated than the mRNA in these hearts (Fig. 1D). *DWORF* mRNA was also down-regulated in ischemic failing human hearts, which potentially links changes in *DWORF* expression with human heart failure (Fig. 1E).

We investigated the subcellular distribution of DWORF in skeletal muscle fibers by electroporation of a green fluorescent protein (GFP)–DWORF expression vector into the flexor digitorum brevis muscle of the mouse foot (¹⁹). Multiphoton excitation microscopy to simultaneously visualize GFP and myosin (using second harmonic generation) showed that GFP-DWORF localizes in an alternating pattern with myosin (Fig. 2A), a distribution consistent with the location of the SR. GFP-SLN and GFP-PLN were individually expressed in the flexor digitorum brevis muscle for comparison. The apparent co-localization of GFP-DWORF, GFP-SLN, and GFP-PLN was striking, including transverse and lengthwise striations typical of SR. The sub-cellular distribution of GFP-DWORF in transfected COS7 cells also overlaps with that of mCherry-SERCA1 in the endoplasmic reticulum (ER) and perinuclear regions (Fig. 2B).

Because GFP-DWORF colocalizes to the SR with SERCA, we tested whether the two proteins physically interact. COS7 cells were cotransfected with GFP or GFP-DWORF and Myc-tagged SERCA1, 2a, 2b, 3a, or 3b. Immunoprecipitation with a GFP antibody coprecipitated GFP-DWORF with all isoforms of SERCA but did not pull down SERCA in GFP transfected samples lacking DWORF (Fig. 2C). We next examined whether coexpression of DWORF with SERCA would affect complex formation between SERCA and PLN, SLN, or MLN. Indeed, we observed a reduction in the binding of hemagglutinin (HA) epitope–tagged peptides HA-PLN, -SLN, and -MLN with SERCA when coexpressed with GFP-DWORF (Fig. 2D and fig. S5), which suggested that binding of DWORF and PLN, SLN, or MLN to SERCA is mutually exclusive. We mutated residues on the M6 transmembrane helix of SERCA1, which are known to interact with PLN, and performed pull-down experiments (²⁰). We observed a reduction in SERCA interaction with GFP-DWORF comparable to that of GFP-PLN, which suggested that both peptides bind to similar regions of the SERCA pump (fig. S6) (²⁰). Coexpression of Myc-SERCA2a with various ratios of GFP-DWORF and GFP-PLN followed by immunoprecipitation with Myc-specific antibody (anti-Myc) and immunoblotting with GFP-specific antibody indicated that DWORF and PLN have similar binding affinities for SERCA (fig. S7).

To assess the functions of DWORF in vivo, we generated mouse models of gain and loss of function. DWORF overexpression in the heart was achieved by expressing untagged DWORF under the control of the cardiomyocyte-specific α MHC promoter in transgenic mice. Two transgenic (Tg) founders that overexpressed the protein were selected for further studies. Other proteins involved in Ca^{2+} handling were largely unaffected in these transgenic mice (figs. S8 and S9).

We used the CRISPR/Cas9 system to disrupt the coding frame of *Dwarf* in mice. A single-guide RNA (gRNA) was designed to target the coding sequence of exon 2 before the transmembrane region (Fig. 3A). Original generation F_0 pups were screened for indels, and a founder with a 2–base pair (2-bp) insertion that disrupts the ORF after codon 16 was chosen for further analysis. Heterozygous *Dwarf* knockout (KO) mice yielded homozygous mutant offspring at expected Mendelian ratios. Western blots of ventricular and soleus muscle probed with DWORF-specific antibody showed that the DWORF protein was eliminated in muscle tissues of homozygous mutant mice (Fig. 3B). To our surprise, the *Dwarf* transcript was up-regulated about fourfold in the *Dwarf*KO tissue (fig. S10A), which suggested a potential feedback mechanism to enhance *Dwarf* expression. Several notable RNA transcripts were not changed in *Dwarf*KO mice, including those encoding the Ca^{2+} -handling proteins SERCA2 and PLN and the cardiac stress markers *Myh7* and atrial natriuretic peptide (*Nppa*). Western blot analysis of heart (fig. S10B) and soleus muscle (fig. S10C) homogenates revealed no detectable changes in protein expression level, phosphorylation state (fig. S11), or oligomerization of major Ca^{2+} -handling proteins.

We examined whether Ca^{2+} flux was altered in adult cardiomyocytes from wild-type (WT), α MHC-DWORF Tg, and *Dwarf*KO mice using the fluorescent Ca^{2+} indicator dye, fluo-4. Isolated cardiomyocytes were loaded with fluo-4, mounted on a temperature-controlled perfusion chamber, and electrically stimulated at 0.5 Hz to initiate intracellular Ca^{2+} transients, which were monitored by epifluorescence. Peak systolic Ca^{2+} transient amplitude and SR Ca^{2+} load were significantly increased in Tg myocytes (Fig. 3, C and D). The pacing-induced Ca^{2+} transient decay rate was significantly enhanced in the Tg myocytes of both α MHC-DWORF Tg lines (Fig. 3E and fig. S12), which suggested that SERCA is more active in these cells (i.e., has a lower tau value). The decay rate of caffeine-induced Ca^{2+} transients was unchanged in Tg myocytes, which indicates that the activity of the $\text{Na}^+/\text{Ca}^{2+}$ exchanger (NCX) is not altered (fig. S13A). Tg myocytes had higher baseline measurements of contractility—as measured by fractional shortening, peak Ca^{2+} transient amplitude, and Ca^{2+} transient decay rate—and responded less to β -adrenergic stimulation by isoproterenol, likely because they function at close to maximally active levels under baseline conditions (figs. S12 and S13, and table S1). In the absence of increased protein abundance of SERCA or changes in other known Ca^{2+} handling proteins, these findings indicate that SERCA activity is increased in muscle cells overexpressing DWORF.

The effect of *Dwarf* ablation on skeletal muscle contractile function was assessed by measuring twitch force at multiple stimulation frequencies in isolated soleus muscles from WT and KO mice (²¹). We did not observe significant differences in peak muscle force between genotypes and saw no differences in relaxation rates at low, non-tetanic stimulation frequencies; however, at tetanus-inducing frequencies, relaxation rates were significantly

slowed in *Dwarf*KO muscles after tetanus (Fig. 3F). The effect on posttetanic relaxation times may suggest that *Dwarf* expression is particularly beneficial for recovery from periods of prolonged contraction and Ca^{2+} release.

Oxalate-supported Ca^{2+} -dependent Ca^{2+} -uptake measurements in muscle homogenates provide a direct quantification of SERCA enzymatic activity (21, 22). We used this technique to measure SERCA activity in hearts of WT, Tg, and KO mice. Hearts overexpressing DWORF showed an apparent increase in SERCA activity at lower concentrations of Ca^{2+} substrate in both of our transgenic lines quantified as a higher affinity of SERCA for Ca^{2+} (reduction in K_{Ca}), and *Dwarf*KO hearts exhibited a less obvious, but still significant, decrease in the affinity of SERCA for Ca^{2+} , as indicated by an increase in K_{Ca} (Fig. 4A, fig. S14A, and table S2). We did not observe changes in the maximal rate of Ca^{2+} pump activity (V_{max}) in any of our genotypes (table S2). Because DWORF is most abundant in the slow-twitch soleus muscle group, we also measured SERCA activity in soleus homogenates from WT and KO mice and used quadriceps muscles as a control, because DWORF is not expressed in this muscle group. Analysis of homogenates from the soleus muscle of *Dwarf*KO mice revealed a decreased apparent affinity of SERCA for Ca^{2+} as compared with homogenates from WT muscles (Fig. 4B and table S3). These differences were not observed in quadriceps muscle (figs. S14B and table S4).

To determine whether DWORF directly activates SERCA or does so through displacement of its endogenous inhibitors, we cotransfected COS7 cells with SERCA2a and DWORF in the presence or absence of PLN, SLN, and MLN (4). We found that coexpression of DWORF alone with SERCA2a did not change the apparent affinity of SERCA for Ca^{2+} , but it relieved the inhibition by PLN in a dose-dependent manner (fig. S15). Threefold overexpression of DWORF was sufficient to return SERCA activity to baseline levels when coexpressed with PLN, SLN, or MLN (fig. S16). These results indicate that DWORF counteracts the effect of inhibitory peptides rather than directly stimulating SERCA pump activity, which is consistent with the lack of primary sequence similarity between DWORF and SERCA inhibitors (fig. S17).

Based on gain- and loss-of-function studies, our results demonstrate that DWORF enhances SR Ca^{2+} uptake and myocyte contractility through its displacement of the inhibitory peptides PLN, SLN, and MLN from SERCA (Fig. 4C). Because DWORF increases the activity of the SERCA pump, it represents an attractive means of enhancing cardiac contractility in settings of heart disease. Finally, our results underscore the likelihood that many transcripts currently annotated as noncoding RNAs encode peptides with important biological functions. These small peptides may evolve rapidly as singular functional domains that fine-tune the activities of larger preexisting molecular complexes, rather than having intrinsic biologic effects themselves. In this regard, small peptides may be uniquely suited to act as key factors in evolutionary adaptation and speciation.

Supplementary Material

Refer to Web version on PubMed Central for supplementary material.

Acknowledgments

We thank C. Long for advice and expertise, N. Beetz for cDNA, J. Cabrera for graphics, S. Johnson for technical support, and the University of Texas Southwestern Medical Center Live Cell Imaging Core Facility under the direction of K. Luby-Phelps. This work was supported by grants from the NIH (HL-077439, HL-111665, HL-093039, DK-099653, U01-HL-100401, and AR-063182), Fondation Leducq Networks of Excellence, Cancer Prevention and Research Institute of Texas, and the Robert A. Welch Foundation (grant 1-0025 to E.N.O.). B.R.N. was supported by a National Institute of Arthritis and Musculoskeletal Diseases, NIH, Ruth L. Kirschstein National Research Service Award (NRSA) (F30AR067094).

References

1. Bers DM. *Nature*. 2002; 415:198–205. [PubMed: 11805843]
2. MacLennan DH, Asahi M, Tupling AR. *Ann N Y Acad Sci*. 2003; 986:472–480. [PubMed: 12763867]
3. Kranias EG, Hajjar RJ. *Circ Res*. 2012; 110:1646–1660. [PubMed: 22679139]
4. Anderson DM, et al. *Cell*. 2015; 160:595–606. [PubMed: 25640239]
5. Bal NC, et al. *Nat Med*. 2012; 18:1575–1579. [PubMed: 22961106]
6. Magny EG, et al. *Science*. 2013; 341:1116–1120. [PubMed: 23970561]
7. Dorn GW 2nd, Molkentin JD. *Circulation*. 2004; 109:150–158. [PubMed: 14734503]
8. Slavoff SA, et al. *Nat Chem Biol*. 2013; 9:59–64. [PubMed: 23160002]
9. Frith MC, et al. *PLOS Genet*. 2006; 2:e52. [PubMed: 16683031]
10. Nelson BR, Anderson DM, Olson EN. *Circ Res*. 2014; 114:18–20. [PubMed: 24385504]
11. Lin MF, Jungreis I, Kellis M. *Bioinformatics*. 2011; 27:i275–i282. [PubMed: 21685081]
12. Xie C, et al. *Nucleic Acids Res*. 2014; 42(D1):D98–D103. [PubMed: 24285305]
13. Sonnhammer EL, von Heijne G, Krogh A. *Proc Int Conf Intell Syst Mol Biol*. 1998; 6:175–182. [PubMed: 9783223]
14. Krogh A, Larsson B, von Heijne G, Sonnhammer EL. *J Mol Biol*. 2001; 305:567–580. [PubMed: 11152613]
15. Goujon M, et al. *Nucleic Acids Res*. 2010; 38(Web Server):W695–W699. [PubMed: 20439314]
16. Guido AN, Campos GE, Neto HS, Marques MJ, Minatel E. *Anat Rec (Hoboken)*. 2010; 293:1722–1728. [PubMed: 20730859]
17. Schiaffino S, Reggiani C. *Physiol Rev*. 2011; 91:1447–1531. [PubMed: 22013216]
18. Molkentin JD, et al. *Cell*. 1998; 93:215–228. [PubMed: 9568714]
19. Nelson BR, et al. *Proc Natl Acad Sci U S A*. 2013; 110:11881–11886. [PubMed: 23818578]
20. Asahi M, Kimura Y, Kurzydowski K, Tada M, MacLennan DH. *J Biol Chem*. 1999; 274:32855–32862. [PubMed: 10551848]
21. Tupling AR, et al. *Am J Physiol Cell Physiol*. 2011; 301:C841–C849. [PubMed: 21697544]
22. Davis BA, Schwartz A, Samaha FJ, Kranias EG. *J Biol Chem*. 1983; 258:13587–13591. [PubMed: 6227613]

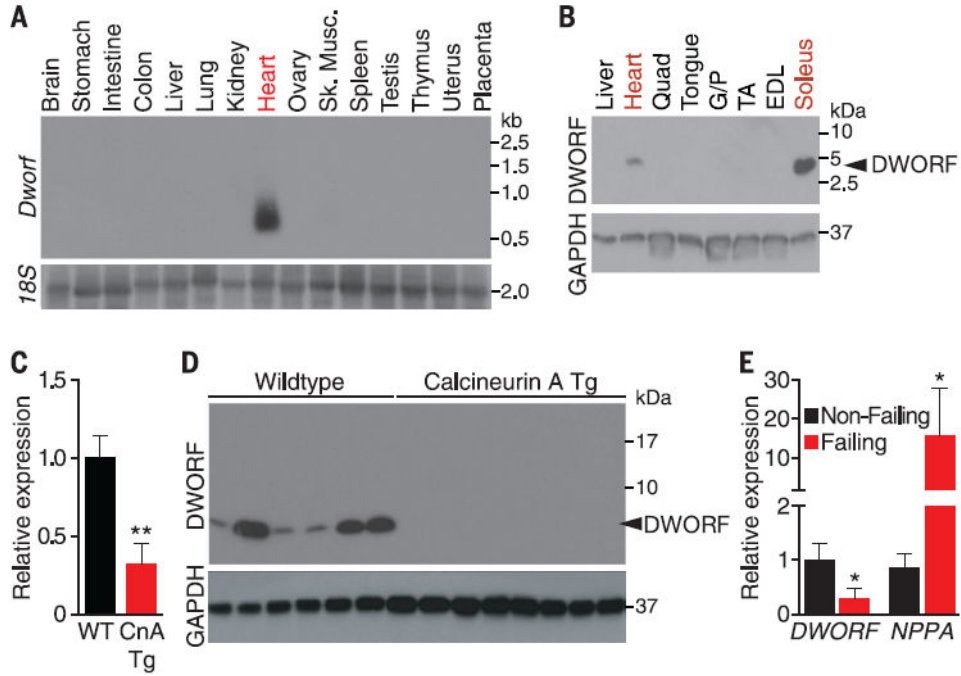


Fig. 1. Muscle-specific expression of the DWORF peptide

(A) Northern blot of adult mouse tissues showing *Dworf* RNA expression. (B) Western blot of adult mouse tissues with the DWORF-specific antibody reveals a single band at the predicted size of 3.8 kD. Quad, quadriceps; G/P, gastrocnemius/plantaris; TA, tibialis anterior; EDL, extensor digitorum longus. (C) Detection of *Dworf* RNA by qRT-PCR in 6-month-old WT and α MHC-CnA mice. Mean \pm SEM; WT, $n = 4$; Tg, $n = 5$. (D) Western blot analysis of heart homogenates from WT and α MHC-calcineurin mice immunoblotted with DWORF-specific antibody. (E) qRT-PCR analysis of human ischemic heart failure tissue showing reduced *DWORF* mRNA in failing hearts, whereas atrial natriuretic peptide (*NPPA*) is significantly increased. Means \pm SEM; nonfailing, $n = 8$; failing, $n = 8$.

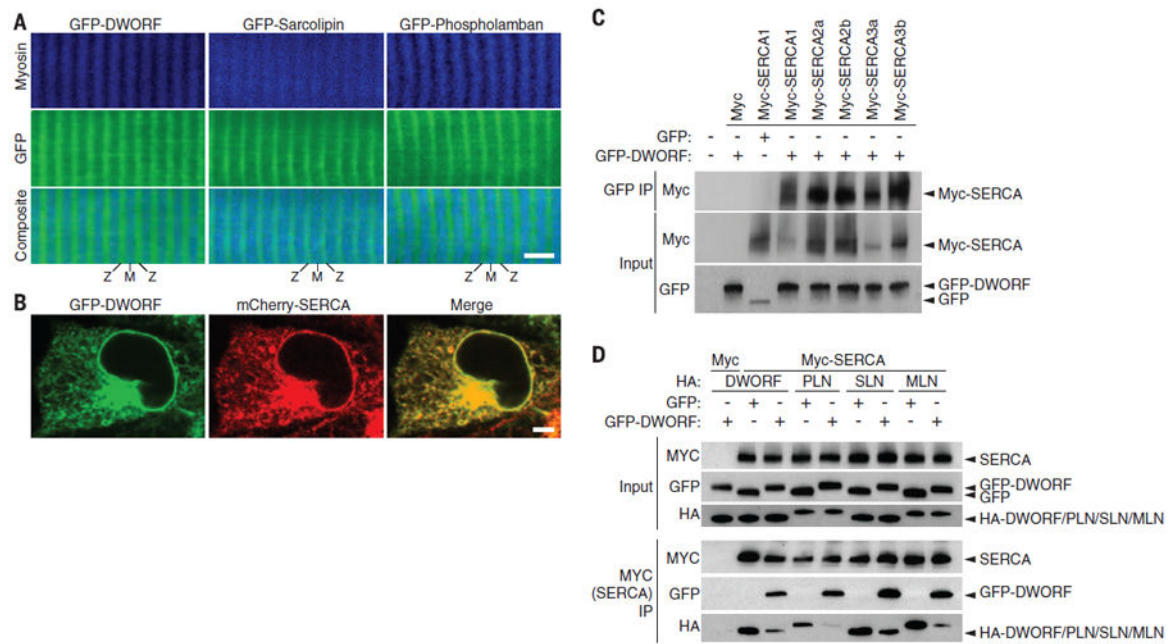


Fig. 2. SR localization and association of DWORF with SERCA

(A) Two-photon scanning confocal microscopy of the flexor digitorum brevis muscle of adult mice after *in vivo* electroporation of plasmids encoding GFP-DWORF, GFP-PLN, or GFP-SLN indicates that DWORF localization closely resembles that of SR proteins PLN and SLN (M, M-line; Z, Z-line; scale bar, 5 μ m). (B) Colocalization of GFP-DWORF and mCherry-SERCA in transfected COS7 cells (scale bar, 5 μ m). (C) Coimmunoprecipitation experiments in transfected COS7 cells using GFP-DWORF and Myc-tagged SERCA isoforms. IP, immunoprecipitation. (D) Immunoprecipitation of Myc-SERCA from lysates of COS7 cells transfected with equal amounts of HA-DWORF, -PLN, -SLN, or -MLN and Myc-SERCA with fivefold overexpression of either GFP or GFP-DWORF. Coexpression of GFP-DWORF reduced the pull-down of HA-tagged peptides in association with SERCA, which indicated that DWORF binding to SERCA excludes binding of PLN, SLN, or MLN.

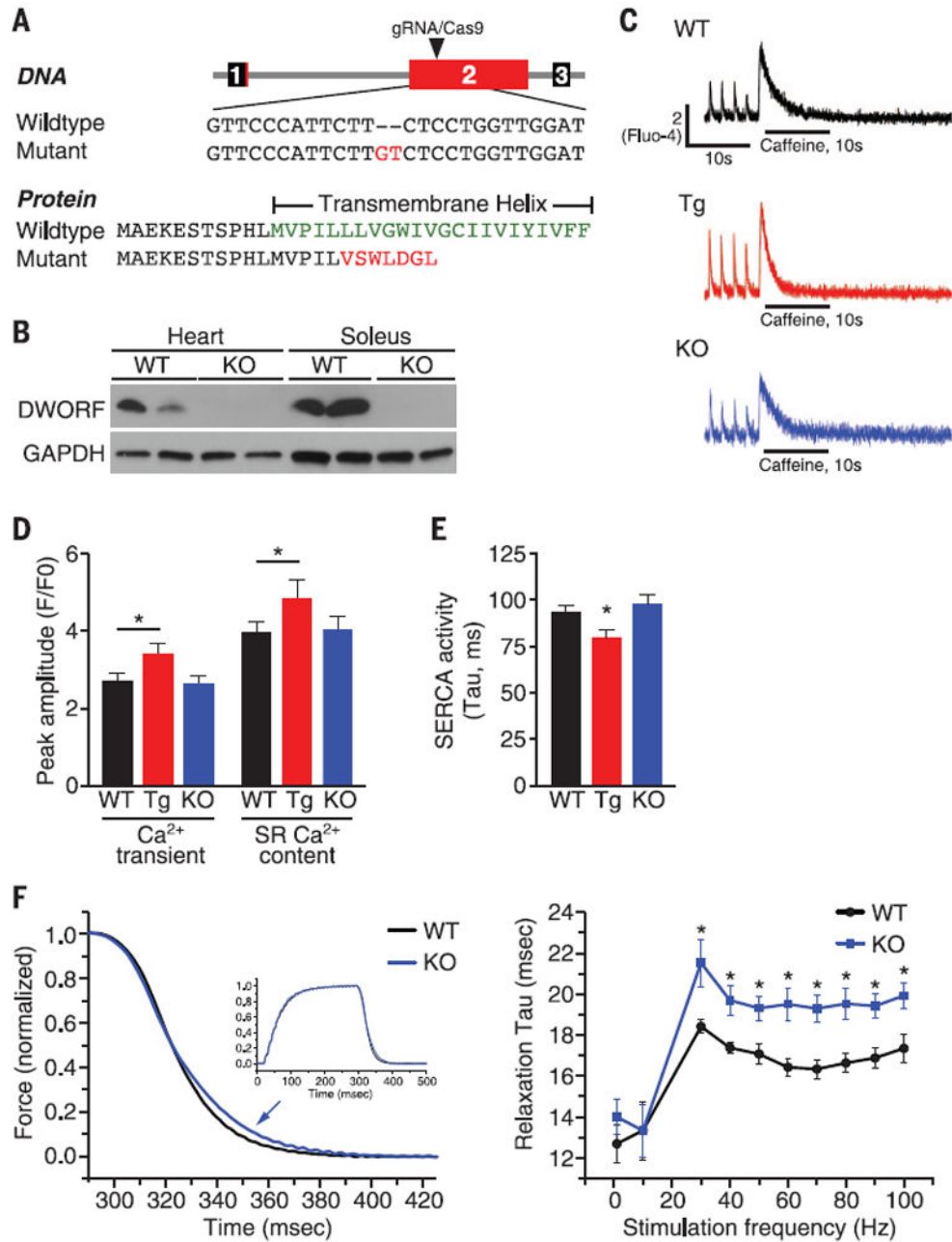


Fig. 3. Consequences of DWORF gain and loss of function

(A) A CRISPR gRNA was generated to target the coding sequence of exon 2. An allele containing a 2-bp insertion was chosen for further experiments. The mutation is expected to produce a truncated protein lacking the transmembrane domain. (B) Western blot showing the absence of DWORF protein in the cardiac ventricle and soleus muscle of *Dwarf* KO mice. (C) Representative Ca²⁺ transients and SR load measurements recorded in fluo-4–loaded cardiomyocytes from WT, α MHC-DWORF (Tg), and *Dwarf* KO mice. (D) Mean amplitude of pacing-induced Ca²⁺ transients in fluo-4–loaded cardiomyocytes from WT, Tg, and KO mice and caffeine-induced Ca²⁺ transients triggered by rapid application of 10 mM

caffeine to quantify SR load. Ca^{2+} signal is shown as fluorescence ratio (F/F_0) with the fluorescence intensity (F) normalized to the minimal intensity measured between 0.5 Hz contractions at diastolic phase (F_0). $P < 0.05$, $n = 6$. (E) Average decay-time constants (τ) of pacing-induced Ca^{2+} transients in WT, Tg, and *Dwarf*KO cardiomyocytes measured by fitting a single exponential to the Ca^{2+} transient decay trace. This parameter is indicative of SERCA activity. $P < 0.05$, $n = 8$. (F) Isometric force was measured from soleus muscles mounted ex vivo and stimulated by 0.2-ms current pulses applied at a range of frequencies. (Left) Force decay was slower in *Dwarf*KO muscles (arrow) after fully fused tetanic contractions as shown for 90 Hz (inset). (Right) Slower relaxation for *Dwarf*KO muscles occurred for stimulus frequencies sufficient to produce twitch fusion (>20 Hz); however, unfused twitches at low frequency showed no difference in relaxation rates. $P < 0.05$, $n = 6$.

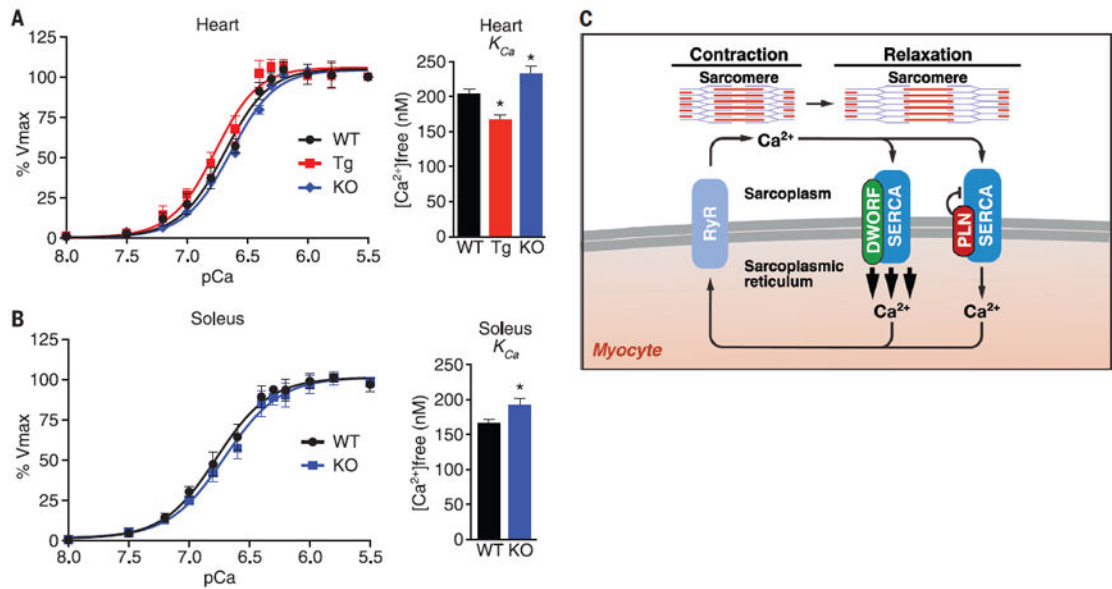


Fig. 4. Effect of DWORF on SERCA activity measured in Ca^{2+} -dependent Ca^{2+} -uptake assays and working model

(A) Ca^{2+} -dependent Ca^{2+} -uptake assays were performed using total homogenates from hearts of WT, α MHC-DWORF (Tg), and *Dwarf*KO mice to directly measure SERCA affinity for Ca^{2+} (K_{Ca}) and SERCA activity. Mean K_{Ca} values from $n = 8$ hearts of each genotype (bar graphs). $P < 0.05$. (B) Ca^{2+} -dependent Ca^{2+} -uptake assays were performed using total homogenates from soleus muscles of WT and *Dwarf*KO mice. Mean K_{Ca} values from mice of each genotype (bar graphs). $P < 0.05$, $n = 8$. (C) Working model for DWORF function.